

Chemical Reaction Effect on MHD Casson Fluid Flow with Newtonian Heating and Heat Source over a Vertical Plate

Shalini Jain¹, Suman Sharma²

^{1,2}Department of Mathematics, University of Rajasthan, Jaipur-302004, INDIA.

Abstract-This study investigates the effects of chemical reaction, Soret, Dufour and Newtonian heating on MHD convective slip flow of Casson fluid over a vertical plate in the presence of non-Darcy porous medium with heat generation or absorption. Using similarity transformations, the governing non-linear coupled PDE are transformed into the coupled ODE. The transformed equations have been solved by BVP4C method using MATLAB software. The physical aspects of the fluid flow and heat transfer have been discussed and presented graphically for various parameter such as Casson fluid parameter, Reynolds number, velocity slip parameter, Grashof number, Biot number, Forchheimer number, Soret number, Dufour number, Prandtl number and chemical reaction parameter.

keywords: Casson fluid, MHD, velocity slip, heat generation or absorption, Soret effect, Dufour effect, Newtonian heating, Chemical reaction.

Introduction

In recent years, non-Newtonian fluid have attracted more attention due to its huge range of applications in industry and engineering. Casson fluid an example of non-Newtonian fluid, is a shear thinning liquid, which exhibits yield stress was introduced by Casson in 1959. It have prominence role in biological, chemical, medical and engineering field. Many researchers have studied flow of Casson fluid on various geometries. Arthur et al. [1] analyzed chemical reaction with magnetic field on the Casson fluid over a vertical porous medium. Jain and Gupta [2] studied heat transfer of Casson fluid flow along vertical sheet in porous medium. Thermal diffusion and chemical reaction influence over vertical porous plate on MHD Casson fluid studied by Kodi et al. [3]. Raj et al. [4] analyzed Casson fluid flow towards vertical plate through porous medium with heat source/sink. Reddy et al. [5] examined Casson fluid flows in the existence of diffusion effects over vertical porous plate in conducting field. Aman and Ishak [6] studied boundary layer flow over a vertical plate with convective boundary condition. Mustafa et al.[7] investigated casson fluid flow over moving flat plat.

Many researchers have carried out their attention to addition of velocity slip condition rather than no slip condition at wall. Ramesh and Devakar [8] studied Couette, Poiseuille, and generalized Couette flows with slip boundary conditions on Casson fluid in between the parallel plates. Kumar et al.[9] Studied slip velocity with heat generation in a non-Darcy porous medium on a Casson fluid flow. Ullah et al. [10] investigated Newtonian heating and velocity slip effect on Casson fluid over nonlinearly stretching sheet with free convection. Gogulapati et al. [11] studied slip effect on temperature, velocity and concentration on mixed convective boundary layer flow over a vertical plate. Obalalu [12] discussed analytical expressions of hydromagnetic, oscillatory, radiative non-Newtonian Casson fluid in a porous medium with slip boundary conditions. Seth et al. [13] investigated flow of Casson fluid over vertical plate through non-Darcy porous medium.

In Newtonian heating where the heat transfer from surface is directly proportional to the local surface temperature. Due to its practical applications researchers studied effects of Newtonian heating on different mathematical models. Merkin [14] studied convection boundary layer flow with Newtonian heating over vertical surface. Khan D. et al.[15] analyzed Casson fluid flow of convection flow over moving vertical plate in a porous medium with magnetic field, chemical reaction, heat generation and Newtonian heating. Devi et al. [16] considered MHD Casson liquid over infinite vertical porous channel with Newtonian heating. Manjula and Sekhar [17] investigated MHD Casson fluid flow with Newtonian heating.

Dufour or diffusion-thermo effect is an energy flux caused by a composition gradient, where Soret or thermal-diffusion effect is an mass fluxes created by temperature gradients had taken much attention. Jain and Parmar [18] investigated transfer of heat and mass with heat source and Dufour effect on casson fluid flow. Moorthy and Senthilvadivu [19] analyzed natural convection flow in porous medium with variable viscosity, Soret and Dufour effects. Reddy and Janardhan [20] studied Soret Dufour effects over vertical plate with chemical reaction and radiation. Alam and Rahman [21] Investigated numerically the Soret and Dufour effects on MHD free convection and mass transfer flow over vertical plate in a porous medium.

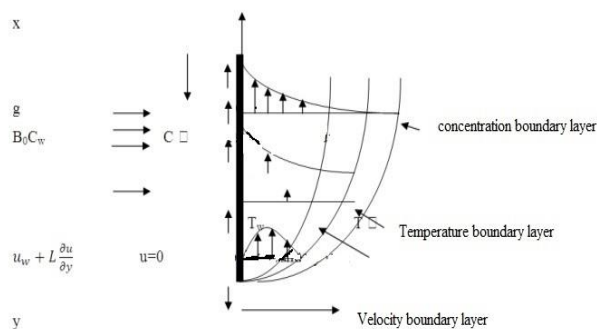
Motivated by the above literature the present study is focused on numerical solution of effect of heat generation or absorption, Newtonian heating, Soret, Dufour and chemical reaction on MHD Casson fluid flows in non-Darcy porous medium over a vertical plate with velocity slip. Using similarity transformations, the governing non-linear coupled PDE are transformed into the

system of coupled ODE and then solved by a MATLAB boundary value problem solver called bvp4c. The features of the fluid flow are analyzed graphically and tabulated for various controlling parameter. The physical aspects are discussed in details.

Mathematical Formulation

In the present paper, we consider a two dimensional steady incompressible, chemically reacting Casson fluid flow in non- Darcy porous medium over a vertical plate.

Let the x-axis along the direction of the plate and it is assumed that the y axis is normal to it. The fluid occupies the half space $y>0$. Let the plate and the fluid are at the same temperature T and the fluid concentration level is same everywhere. The plate temperature and concentration are raised to $T_w(>T_\infty)$ and $C_w(>C_\infty)$ instantly at time $t>0$, After that maintained constant. C_∞ and T_∞ are the concentration and temperature respectively outside the boundary layer.



Let the rheological equation of Casson fluid can be written as

$$\tau_{ij} = \left(\mu_b + \frac{P_y}{\sqrt{2\pi}} \right) 2e_{ij}, \quad \text{where } \pi > \pi_c \quad (1)$$

$$\tau_{ij} = \left(\mu_b + \frac{P_y}{\sqrt{2\pi_c}} \right) 2e_{ij}, \quad \text{where } \pi < \pi_c \quad (2)$$

P_y : Yield Stress, $P_y = \frac{\mu_b}{\beta} \sqrt{2\sqrt{\pi}}$

where, μ_b is plastic dynamic viscosity of fluid ($\pi = e_{ij}e_{ij}$).

The Casson fluid flow, where $\pi > \pi_c$ and

$$\mu = \mu_b + \frac{P_y}{\sqrt{2\pi}} \quad (3)$$

The relevant governing equation to the problem are given by:

Continuity equation

$$\frac{\partial u}{\partial x} + \frac{\partial v}{\partial y} = 0 \quad (4)$$

Momentum equation

$$u \frac{\partial u}{\partial x} + v \frac{\partial u}{\partial y} = \nu \left(1 + \frac{1}{\beta} \right) \frac{\partial^2 u}{\partial y^2} + g\beta_T (T - T_\infty) + g\beta_c (C - C_\infty) - \frac{\sigma B_0^2 u}{\rho} - \frac{\nu}{k'} u - \frac{bu^2}{k'} \quad (5)$$

Energy equation

$$u \frac{\partial T}{\partial x} + v \frac{\partial T}{\partial y} = \alpha \frac{\partial^2 T}{\partial y^2} + \frac{Q_1^*(x)}{\rho c_p} (T - T_\infty) + \frac{Q_2^*(x)}{\rho c_p} (C - C_\infty) + \frac{D_m k_T}{c_p c_s} \frac{\partial^2 C}{\partial y^2} \quad (6)$$

Concentration equation

$$u \frac{\partial C}{\partial x} + v \frac{\partial C}{\partial y} = D_m \frac{\partial^2 C}{\partial y^2} + \frac{D_m k_T}{T_m} \frac{\partial^2 T}{\partial y^2} - k_0 (C - C_\infty) \quad (7)$$

The appropriate boundary condition as per formulation are prescribed as

$$\begin{aligned} \text{at } y=0 \quad u &= u_w + L \frac{\partial u}{\partial y}, v = -v_0, & -k \frac{\partial T}{\partial y} &= h_f(T_w - T), C = C_w \\ \text{at } y \rightarrow \infty \quad u &= 0, T \rightarrow T_\infty, C \rightarrow C_\infty, \end{aligned} \quad (8)$$

Here, kinematic viscosity is ν , $\beta = \frac{\mu b}{\rho \nu} \sqrt{2\pi} c$ is non-Newtonian Casson parameter, $v_0 > 0$ is the velocity of suction and $v_0 < 0$ is the velocity of injection, α is the thermal diffusivity, D_m is mass diffusivity, T is the temperature of the fluid, T_w is temperature at the surface, T_∞ is free stream temperature, C is the concentration of the fluid, C_w is concentration at the surface, C_∞ is free stream concentration, $Q_1^*(x)$ is coefficient of heat generation of temperature, $Q_2^*(x)$ is coefficient of proportionality for the absorption, g is gravitational acceleration, σ is electrical conductivity, ρ is the fluid density, b is the Forchheimer constant, C_p is specific heat, C_s is Concentration susceptibility, k_0 is the chemical reaction rate constant, L is the initial value of the velocity slip factor.

Stream function $\psi(x, y)$ which satisfies the equation of continuity such that

$$u = \frac{\partial \psi}{\partial y} \quad \text{and} \quad v = -\frac{\partial \psi}{\partial x} \quad (9)$$

now, we are introducing the following similarity

$$\eta = y \sqrt{\frac{u_w}{\nu x}}, \quad \psi(\eta) = \sqrt{(u_w \nu x)} f(\eta) \quad (10)$$

$$f(\eta) = \frac{\psi(\eta)}{\sqrt{(u_w \nu x)}} \quad (11)$$

The dimensionless quantities for temperature and concentration are introduced:

$$\theta(\eta) = \frac{T - T_\infty}{T_w - T_\infty} \quad (12)$$

$$\phi(\eta) = \frac{C - C_\infty}{C_w - C_\infty} \quad (13)$$

Using non-dimensional variables eqs. (4)-(8) are reduced into non-linear ODE which are written as follows:

$$\left(1 + \frac{1}{\beta}\right) f''''(\eta) + Gr \theta(\eta) + Gc \phi(\eta) - (M + f'(\eta))f'(\eta) - \frac{1}{Da Re_x} f'(\eta) - \frac{Fs}{Da} f'^2 + f(\eta)f''(\eta) = 0 \quad (14)$$

$$\frac{1}{Pr} \theta''(\eta) + f(\eta)\theta'(\eta) + Q_1\theta(\eta) + Q_2\phi(\eta) + Du \phi''(\eta) = 0 \quad (15)$$

$$\frac{1}{Sc} \phi''(\eta) + f(\eta)\phi'(\eta) - Kr \phi(\eta) + Sr \theta''(\eta) = 0 \quad (16)$$

Reduced boundary conditions are given as :

$$f(0) = f_w, f'(0) = 1 + \lambda f''(0),$$

$$\theta'(0) = r_2(\theta - 1), \phi(0) = 1 \text{ and}$$

$$f' = \theta = \phi = 0 \text{ as } \eta \rightarrow \infty \quad (17)$$

Where the primes denote differentiation with respect to η .

Where

Thermal Grashof number $Gr = \frac{g\beta T(T_w - T_\infty)x}{u_w^2}$, solutal Grashof number $Gc = \frac{g\beta_c(C_w - C_\infty)x}{u_w^2}$, magnetic field parameter $M = \frac{\sigma B_0^2}{a\rho}$, local Darcy number $Da = \frac{k'}{x^2}$, Reynolds number $Re_x = \frac{ax^2}{\nu}$, Forchheimer number $Fs = \frac{b}{x}$, Prandtl number $Pr = \frac{\nu}{\mu}$, heat generation\absorption parameter $Q_1 = \frac{Q_1^*(x)}{a\rho C_p}$, radiation absorption parameter $Q_2 = \frac{Q_2^*(x)(C_w - C_\infty)}{a\rho C_s(T_w - T_\infty)}$, Schmidt number $Sc = \frac{\mu}{D_m}$, chemical reaction parameter $Kr = \frac{k_0}{a}$, Soret Number $Sr = \frac{D_m k T}{T_m \nu} \frac{1}{\nu} \frac{(T_w - T_\infty)}{(C_w - C_\infty)}$, Slip parameter $\lambda = L \sqrt{\frac{a}{\nu}}$, Biot Number $r_2 = \sqrt{\frac{\nu h_f}{a k}}$, Suction (>0) or injection (<0) parameter $f_w = -\frac{v_0(x)}{\sqrt{a\nu}}$.

$$\text{Skin-friction coefficient } C_{fx} = -\frac{\tau_w}{\rho u_w^2}, \text{ Nusselt number } Nu_x = \frac{xq_x}{k(T_w - T_\infty)}, \text{ Sherwood number } Sh_x = \frac{xq_x}{D_m(C_w - C_\infty)}.$$

Using the similarity variables (9)-(13), the resulting equations are

$$\begin{aligned}
 C_{fx} Re_x^{\frac{1}{2}} &= -\left(1 + \frac{1}{\beta}\right) f'''(0), \\
 Nu_x Re_x^{\frac{1}{2}} &= -\theta'(0), \\
 Sh_x Re_x^{\frac{1}{2}} &= -\phi'(0)
 \end{aligned}
 \tag{18}$$

Solution of the Problem:

The coupled ordinary differential equations (14)-(16) together with the transformed boundary conditions (17) are solved by numerical technique called bvp4c, using a MATLAB boundary value problem solver. The skin-friction coefficient C_{fx} local Nusselt number Nu_x and local sherwood number Sh_x which are proportional to $f'''(0)$, $\theta'(0)$ and $\phi'(0)$ respectively are computed and the numerical values are presented in a tabular form.

Results and Discussion:

Figure (2-4) shows the impact of magnetic parameter M on velocity, temperature and concentration profile respectively. By increasing M the concentration of boundary layer increases which retards the fluid flow. Dimension less temperature and concentration increases and velocity decreases with raising the magnetic parameter.

Figure (5-7) displays the effects of the velocity slip parameter λ . It is observed that as the velocity slip parameter increases the slip velocity increases and the fluid velocity decreases. Temperature and concentration profiles increases as the value of the velocity slip parameter increases.

Figure (8-10) shows velocity profile decreases, temperature and concentration profiles increases with non-Newtonian Casson parameter β .

Figure (11-13) represents the effect of Darcy number (Da). Velocity distribution of the fluid decreases, temperature and concentration distribution increases with the influence of Darcy number.

In figure (14-16) It is observed velocity distribution decreases, temperature and concentration increases with an increasing Forchheimer number F_s .

Figure(17-19) shows the effect of suction/injection parameter on velocity, temperature and concentration parameter.

As the chemical reaction parameter (K_r) increases, the rate of interfacial mass transfer increases. Local concentration reduces due to the reaction and thus increases its concentration gradient. Figure (20-22) shows that as the chemical reaction parameter (K_r) increases, velocity, temperature and concentration profiles decreases significantly.

Figure (23-25) illustrate the effect of Biot number r_2 on velocity, temperature and concentration profiles. By increasing Biot number amount of heat which transmitted to the fluid increases, this energizes the boundary layer. As the Biot number increases momentum, temperature and concentration profiles increases significantly.

Influence of Soret and Dufour number is shown in figure (26-28).The values of Soret number S_r and Dufour number D_u are chosen. The product of Soret and Dufour number is constant.

Table 5.1 : Numerical computation of skin friction coefficient $f'''(0)$, local Nusselt number $\theta'(0)$ and local Sherwood number $\phi'(0)$ for $\beta=0.5$, $Re_x=100$, $Gr=0.2$, $Gc=6$, $F_s=0.1$, $Da=0.1$, $Pr=2$, $Q_1=0.1$, $Q_2=0.1$, $Sc=0.2$, $K_r=0.3$, $F_w=0.5$, $M=0.5$.

λ	r_2	D_u	S_r	$-f'''(0)$	$-\theta'(0)$	$-\phi'(0)$
0.0	0.1	0.12	0.5	1.4643	0.7017	0.3941
0.4				0.6756	0.0693	0.3845
0.8				0.4403	0.0686	0.3816
1.0				0.3751	0.0683	0.3808
1.2				0.3267	0.0682	0.3802

1.5	0.1	0.12	0.5	0.2738	0.6802	0.3795
	0.3			0.2728	0.1808	0.3703
	0.5			0.2720	0.2707	0.3630
	0.7			0.2713	0.3440	0.3571
	0.9			0.2708	0.4050	0.3521
1.5	0.1	0.030	2.0	0.2725	0.0705	0.3734
		0.050	1.2	0.2733	0.0701	0.3765
		0.075	0.8	0.2736	0.0694	0.3782
		0.150	0.4	0.2738	0.0670	0.3800
		0.300	0.2	0.2736	0.0620	0.3810
		0.600	0.1	0.2728	0.0518	0.3817

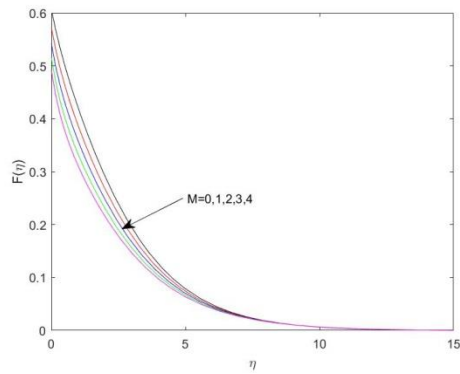


Fig.2. Dimensionless velocity distribution for magnetic parameter M with $\beta=0.5$, $Re_x=100$, $Gr=0.2$, $Gc=6$, $Fs=0.1$, $Da=0.1$, $Pr=2$, $Q1=0.1$, $Q2=0.1$, $Sc=0.2$, $Kr=0.3$, $Sr=0.5$, $Du=0.12$, $\lambda=1.5$, $Fw=0.5$, $r2=0.1$.

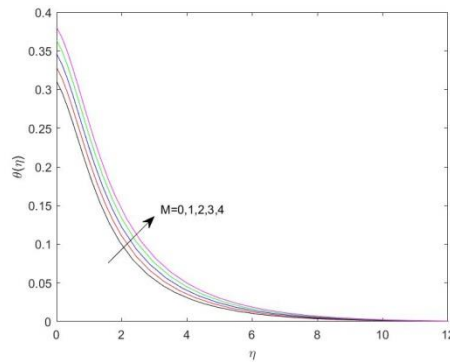


Fig.3. Dimensionless temperature distribution for magnetic parameter M with $\beta=0.5$, $Re_x=100$, $Gr=0.2$, $Gc=6$, $Fs=0.1$, $Da=0.1$, $Pr=2$, $Q1=0.1$, $Q2=0.1$, $Sc=0.2$, $Kr=0.3$, $Sr=0.5$, $Du=0.12$, $\lambda=1.5$, $Fw=0.5$, $r2=0.1$.

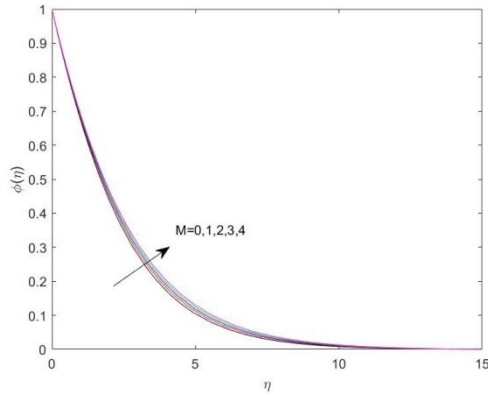


Fig.4. Dimensionless concentration distribution for magnetic parameter M with $\beta=0.5$, $Re_x=100$, $Gr=0.2$, $Gc=6$, $Fs=0.1$, $Da=0.1$, $Pr=2$, $Q1=0.1$, $Q2=0.1$, $Sc=0.2$, $Kr=0.3$, $Sr=0.5$, $Du=0.12$, $\lambda=1.5$, $Fw=0.5$, $r2=0.1$.

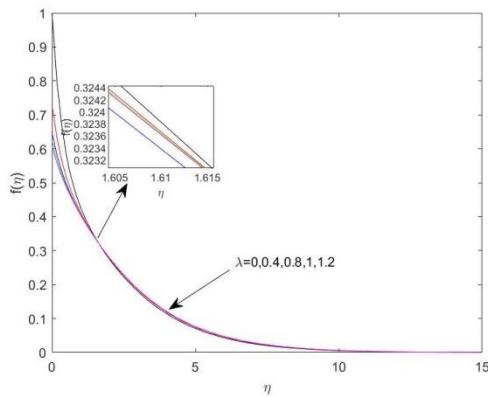


Fig.5. Dimensionless velocity distribution for slip parameter λ with $\beta=0.5$, $Re_x=100$, $Gr=0.2$, $Gc=6$, $Fs=0.1$, $Da=0.1$, $Pr=2$, $Q1=0.1$, $Q2=0.1$, $Sc=0.2$, $Kr=0.3$, $Sr=0.5$, $Du=0.12$, $M=0.5$, $Fw=0.5$, $r2=0.1$

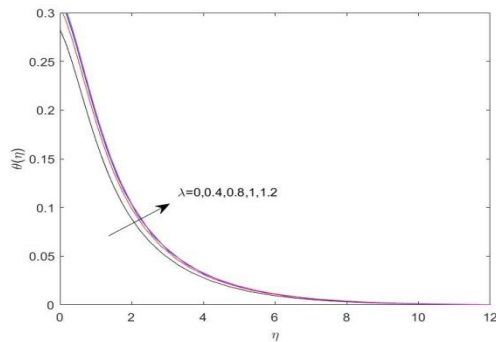


Fig.6. Dimensionless temperature distribution for slip parameter λ with $\beta=0.5$, $Re_x=100$, $Gr=0.2$, $Gc=6$, $Fs=0.1$, $Da=0.1$, $Pr=2$, $Q1=0.1$, $Q2=0.1$, $Sc=0.2$, $Kr=0.3$, $Sr=0.5$, $Du=0.12$, $M=0.5$, $Fw=0.5$, $r2=0.1$

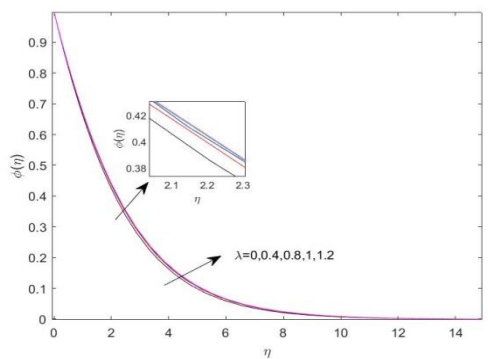


Fig.7. Dimensionless concentration distribution for slip parameter λ with $\beta=0.5$, $Re_x=100$, $Gr=0.2$, $Gc=6$, $Fs=0.1$, $Da=0.1$, $Pr=2$, $Q1=0.1$, $Q2=0.1$, $Sc=0.2$, $Kr=0.3$, $Sr=0.5$, $Du=0.12$, $M=0.5$, $Fw=0.5$, $r2=0.1$ Fig.8. Dimensionless velocity distribution for Casson fluid parameter β with $M=0.5$, $Re_x=100$, $Gr=0.2$, $Gc=6$, $Fs=0.1$, $Da=0.1$, $Pr=2$, $Q1=0.1$, $Q2=0.1$, $Sc=0.2$, $Kr=0.3$, $Sr=0.5$, $Du=0.12$, $\lambda=1.5$, $Fw=0.5$, $r2=0.1$

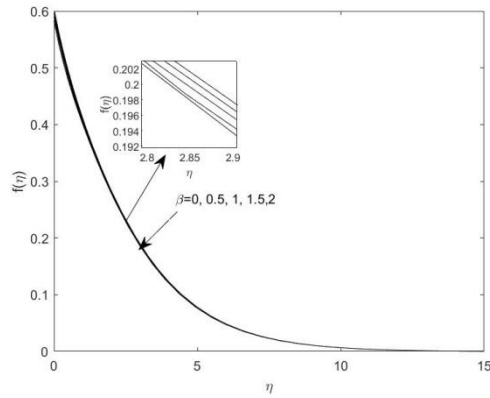


Fig.8. Dimensionless velocity distribution for Casson fluid parameter β with $M=0.5$, $Re_x=100$, $Gr=0.2$, $Gc=6$, $Fs=0.1$, $Da=0.1$, $Pr=2$, $Q1=0.1$, $Q2=0.1$, $Sc=0.2$, $Kr=0.3$, $Sr=0.5$, $Du=0.12$, $\lambda=1.5$, $Fw=0.5$, $r2=0.1$.

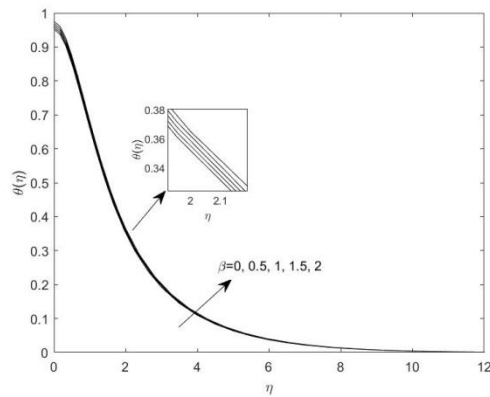


Fig.9. Dimensionless temperature distribution for Casson fluid parameter β with $M=0.5$, $Re_x=100$, $Gr=0.2$, $Gc=6$, $Fs=0.1$, $Da=0.1$, $Pr=2$, $Q1=0.1$, $Q2=0.1$, $Sc=0.2$, $Kr=0.3$, $Sr=0.5$, $Du=0.12$, $\lambda=1.5$, $Fw=0.5$, $r2=0.1$.

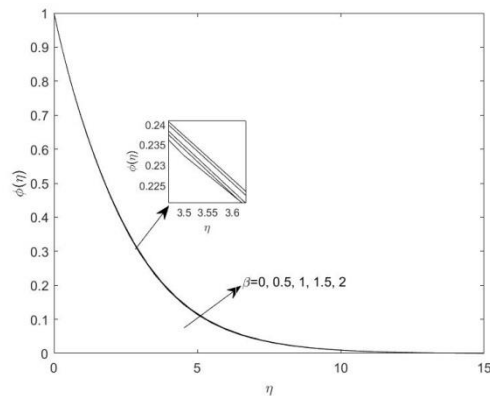


Fig.10. Dimensionless concentration distribution for Casson fluid parameter β with $M=0.5$, $Re_x=100$, $Gr=0.2$, $Gc=6$, $Fs=0.1$, $Da=0.1$, $Pr=2$, $Q1=0.1$, $Q2=0.1$, $Sc=0.2$, $Kr=0.3$, $Sr=0.5$, $Du=0.12$, $\lambda=1.5$, $Fw=0.5$, $r2=0.1$.

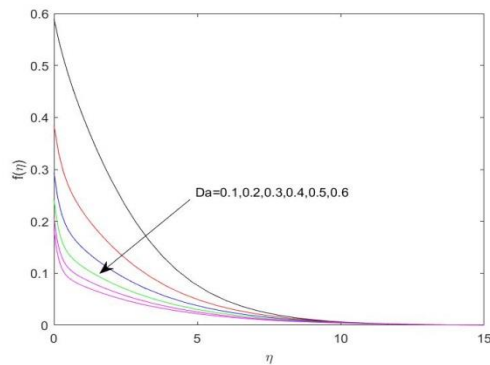


Fig.11. Dimensionless velocity distribution for local Darcy number Da with $\beta=0.5$, $M=0.5$, $Re_x=100$, $Gr=0.2$, $Gc=6$, $Fs=0.1$, $Pr=2$, $Q1=0.1$, $Q2=0.1$, $Sc=0.2$, $Kr=0.3$, $Sr=0.5$, $Du=0.12$, $\lambda=1.5$, $Fw=0.5$, $r2=0.1$.

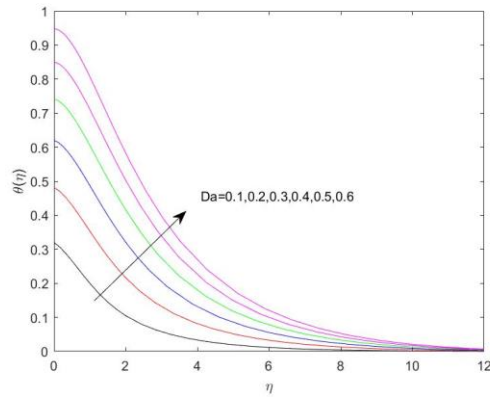


Fig.12. Dimensionless temperature distribution for local Darcy number Da with $\beta=0.5$, $M=0.5$, $Re_x=100$, $Gr=0.2$, $Gc=6$, $Fs=0.1$, $Pr=2$, $Q1=0.1$, $Q2=0.1$, $Sc=0.2$, $Kr=0.3$, $Sr=0.5$, $Du=0.12$, $\lambda=1.5$, $Fw=0.5$, $r2=0.1$.

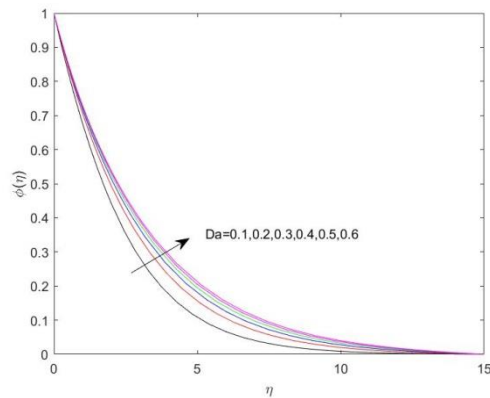


Fig.13. Dimensionless concentration distribution for local Darcy number Da with $\beta=0.5$, $M=0.5$, $Re_x=100$, $Gr=0.2$, $Gc=6$, $Fs=0.1$, $Pr=2$, $Q1=0.1$, $Q2=0.1$, $Sc=0.2$, $Kr=0.3$, $Sr=0.5$, $Du=0.12$, $\lambda=1.5$, $Fw=0.5$, $r2=0.1$.

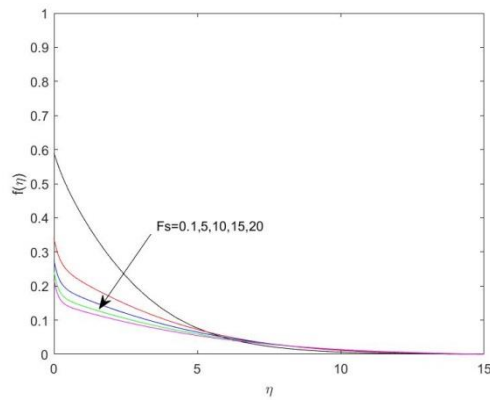


Fig.14. Dimensionless velocity distribution for Forchheimer number Fs with $\beta=0.5$, $M=0.5$, $Re_x=100$, $Gr=0.2$, $Gc=6$, $Da=0.1$, $Pr=2$, $Q1=0.1$, $Q2=0.1$, $Sc=0.2$, $Kr=0.3$, $Sr=0.5$, $Du=0.12$, $\lambda=1.5$, $Fw=0.5$, $r2=0.1$.

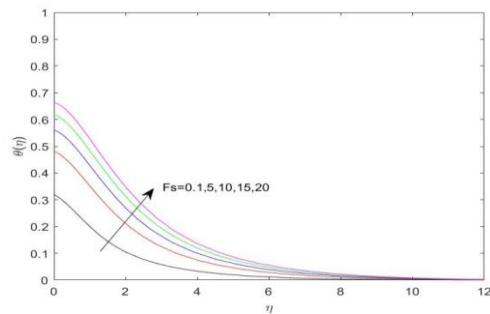


Fig.15. Dimensionless temperature distribution for Forchheimer number Fs with $\beta=0.5$, $M=0.5$, $Re_x=100$, $Gr=0.2$, $Gc=6$, $Da=0.1$, $Pr=2$, $Q1=0.1$, $Q2=0.1$, $Sc=0.2$, $Kr=0.3$, $Sr=0.5$, $Du=0.12$, $\lambda=1.5$, $Fw=0.5$, $r2=0.1$.

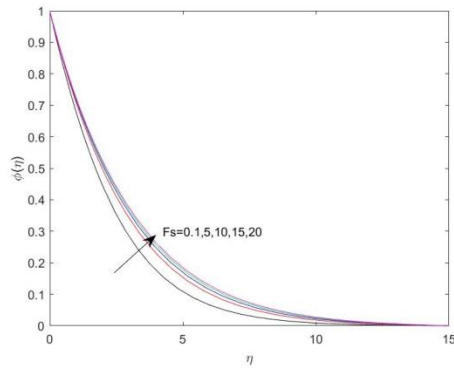


Fig.16. Dimensionless concentration distribution for Forchheimer number F_s with $\beta=0.5, M=0.5, Re_x=100, Gr=0.2, Gc=6, Da=0.1, Pr=2, Q1=0.1, Q2=0.1, Sc=0.2, Kr=0.3, Sr=0.5, Du=12, \lambda=1.5, F_w=0.5, r_2=0.1$.

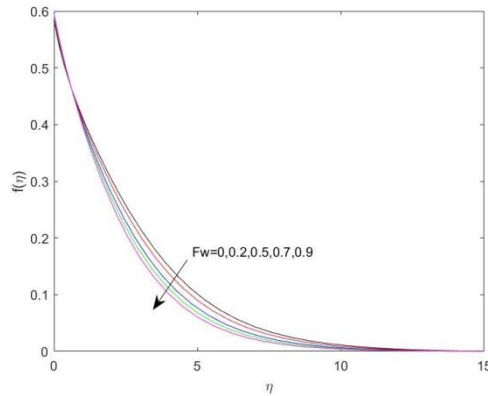


Fig.17. Dimensionless velocity distribution for suction or injection parameter F_w with $\beta=0.5, M=0.5, Re_x=100, Gr=0.2, Gc=6, Da=0.1, Pr=2, Q1=0.1, Q2=0.1, Sc=0.2, Kr=0.3, Sr=0.5, Du=0.12, \lambda=1.5, r_2=0.1$.

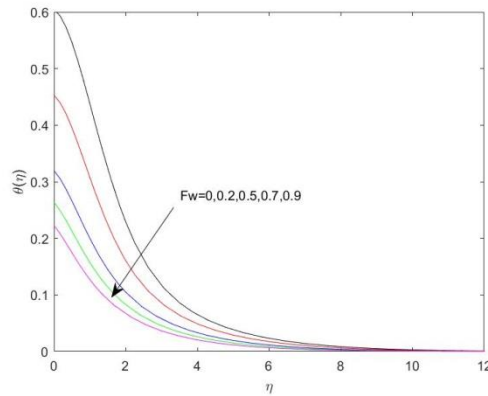


Fig.18. Dimensionless temperature distribution for suction or injection parameter F_w with $\beta=0.5, M=0.5, Re_x=100, Gr=0.2, Gc=6, Da=0.1, Pr=2, Q1=0.1, Q2=0.1, Sc=0.2, Kr=0.3, Sr=0.5, Du=0.12, \lambda=1.5, r_2=0.1$.

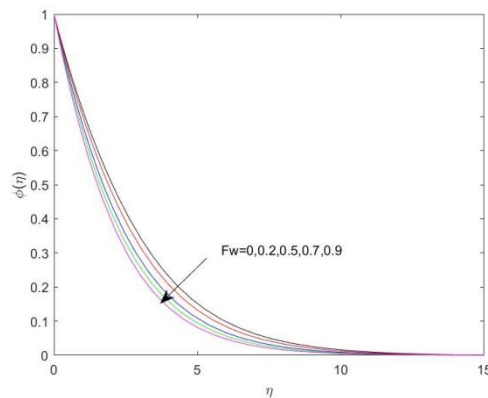


Fig.19. Dimensionless concentration distribution for suction or injection parameter F_w with $\beta=0.5$, $M=0.5$, $Re_x=100$, $Gr=0.2$, $Gc=6$, $Da=0.1$, $Pr=2$, $Q1=0.1$, $Q2=0.1$, $Sc=0.2$, $Kr=0.3$, $Sr=0.5$, $Du=0.12$, $\lambda=1.5$, $r2=0.1$.

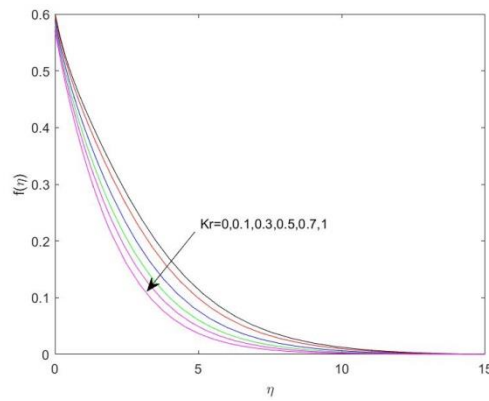


Fig.20. Dimensionless velocity distribution for chemical reaction Kr parameter with $\beta=0.5$, $M=0.5$, $Re_x=100$, $Gr=0.2$, $Gc=6$, $Da=0.1$, $Pr=2$, $Q1=0.1$, $Q2=0.1$, $Sc=0.2$, $Sr=0.5$, $Fs=0.1$, $Du=0.12$, $r2=0.1$, $\lambda=1.5$, $Fw=0.5$, $Fs=0.1$.

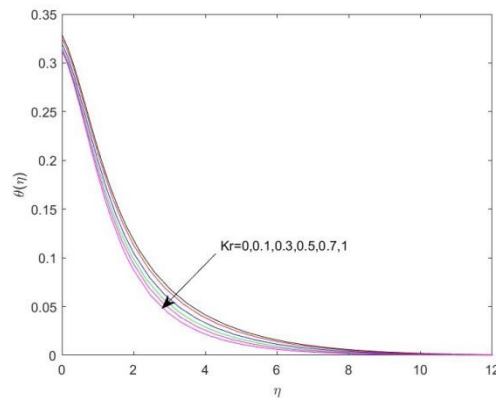


Fig.21. Dimensionless temperature distribution for chemical reaction Kr parameter with $\beta=0.5$, $M=0.5$, $Re_x=100$, $Gr=0.2$, $Gc=6$, $Da=0.1$, $Pr=2$, $Q1=0.1$, $Q2=0.1$, $Sc=0.2$, $Sr=0.5$, $Fs=0.1$, $Du=0.12$, $r2=0.1$, $\lambda=1.5$, $Fw=0.5$.

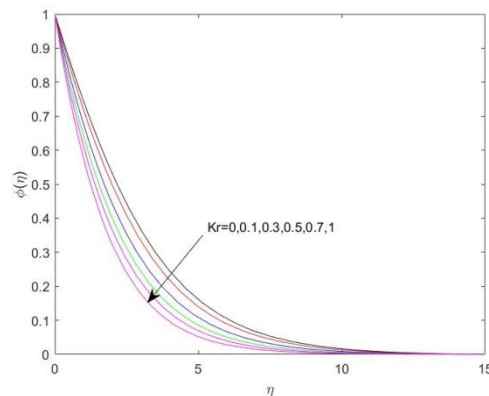


Fig.22. Dimensionless concentration distribution for chemical reaction Kr parameter with $\beta=0.5$, $M=0.5$, $Re_x=100$, $Gr=0.2$, $Gc=6$, $Da=0.1$, $Pr=2$, $Q1=0.1$, $Q2=0.1$, $Sc=0.2$, $Sr=0.5$, $Fs=0.1$, $Du=0.12$, $r2=0.1$, $\lambda=1.5$, $Fw=0.5$, $Fs=0.1$.

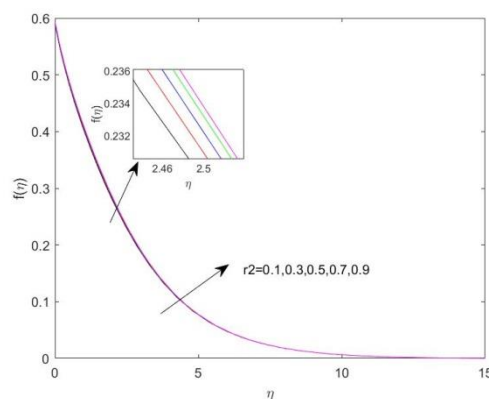


Fig.23. Dimensionless velocity distribution for Biot number r_2 with $\beta=0.5$, $M=0.5$, $Re_x=100$, $Gr=0.2$, $Gc=6$, $Da=0.1$, $Pr=2$, $Q_1=0.1$, $Q_2=0.1$, $Sc=0.2$, $Kr=0.3$, $Sr=0.5$, $Du=0.12$, $\lambda=1.5$, $Fw=0.5$, $Fs=0.1$.

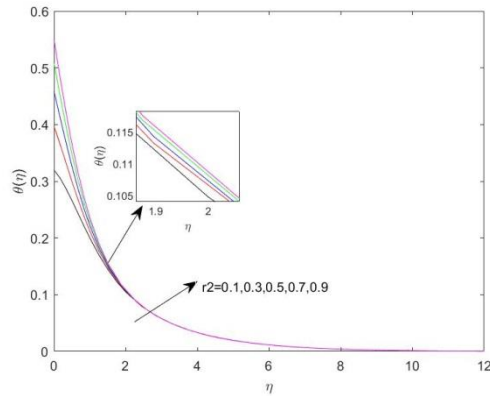


Fig.24. Dimensionless temperature distribution for Biot number r_2 with $\beta=0.5$, $M=0.5$, $Re_x=100$, $Gr=0.2$, $Gc=6$, $Da=0.1$, $Pr=2$, $Q_1=0.1$, $Q_2=0.1$, $Sc=0.2$, $Kr=0.3$, $Sr=0.5$, $Du=0.12$, $\lambda=1.5$, $Fw=0.5$, $Fs=0.1$.

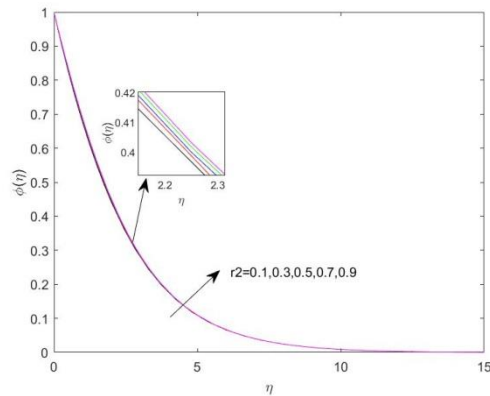


Fig.25. Dimensionless concentration distribution for Biot number r_2 with $\beta=0.5$, $M=0.5$, $Re_x=100$, $Gr=0.2$, $Gc=6$, $Da=0.1$, $Pr=2$, $Q_1=0.1$, $Q_2=0.1$, $Sc=0.2$, $Kr=0.3$, $Sr=0.5$, $Du=0.12$, $\lambda=1.5$, $Fw=0.5$, $Fs=0.1$.

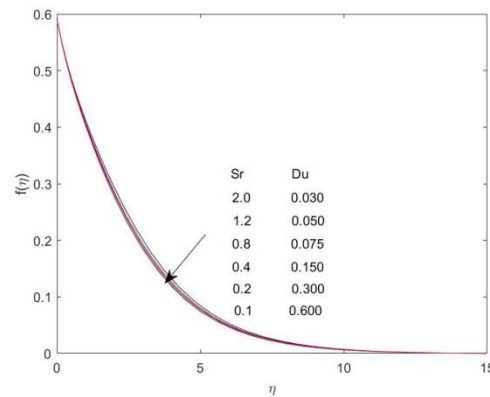


Fig.26. Dimensionless velocity distribution for Soret and Dufour parameter with $\beta=0.5$, $M=0.5$, $Re_x=100$, $Gr=0.2$, $Gc=6$, $Da=0.1$, $Pr=2$, $Q_1=0.1$, $Q_2=0.1$, $Sc=0.2$, $Kr=0.3$, $r_2=0.1$, $\lambda=1.5$, $Fw=0.5$, $Fs=0.1$.

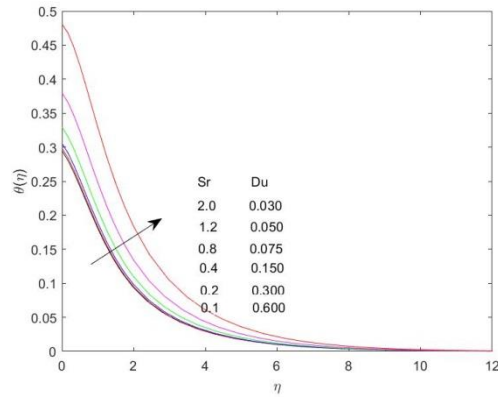


Fig.27. Dimensionless temperature distribution for Soret and Dufour parameter with $\beta=0.5$, $M=0.5$, $Re_x=100$, $Gr=0.2$, $Gc=6$, $Da=0.1$, $Pr=2$, $Q1=0.1$, $Q2=0.1$, $Sc=0.2$, $Kr=0.3$, $r2=0.1$, $\lambda=1.5$, $Fw=0.5$, $Fs=0.1$.

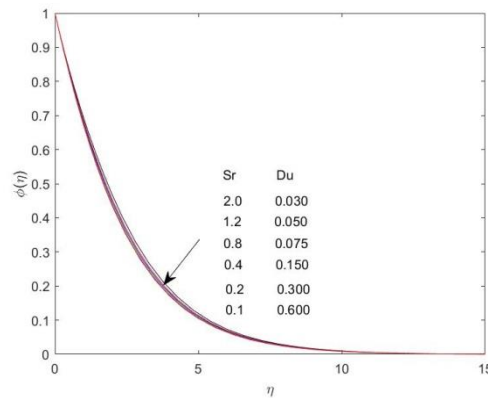


Fig.28. Dimensionless concentration distribution for Soret and Dufour parameter with $\beta=0.5$, $M=0.5$, $Re_x=100$, $Gr=0.2$, $Gc=6$, $Da=0.1$, $Pr=2$, $Q1=0.1$, $Q2=0.1$, $Sc=0.2$, $Kr=0.3$, $r2=0.1$, $\lambda=1.5$, $Fw=0.5$, $Fs=0.1$.

Conclusions

This paper investigates the effect of Soret, Dufour and Newtonian heating on Casson fluid flow over vertical plate in the presence of non-Darcy porous medium with chemical reaction and heat source. The governing equations were solved by bvp4c method using MATLAB software. The results are analyzed and presented graphically. It is observed that:

- As the Biot number increases velocity, temperature and concentration profiles increases.
- Velocity distribution of the fluid increases, temperature and concentration distribution decreases with the influence of increasing Darcy number.
- Velocity distribution decreases, temperature and concentration increases with an increasing Forchheimer number.
- Velocity, temperature and concentration profiles decreases significantly with an increasing chemical reaction parameter.
- Velocity, temperature and concentration profiles decreases with increasing suction or injection parameter.